Bioconjugate Chemistry

ARTICLE

pubs.acs.org/bc

Targeting G-Quadruplex Structure in the Human c-Kit Promoter with Short PNA Sequences

Jussara Amato,[#,†] Bruno Pagano,[#,‡] Nicola Borbone,[†] Giorgia Oliviero,[*,†] Valérie Gabelica,[§] Edwin De Pauw,[§] Stefano D'Errico,[†] Vincenzo Piccialli,[∥] Michela Varra,[†] Concetta Giancola,[⊥] Gennaro Piccialli,[†] and Luciano Mayol[†]

[†]Dipartimento di Chimica delle Sostanze Naturali, Università degli Studi di Napoli Federico II, via D. Montesano 49, 80131, Napoli, Italy

[‡]Dipartimento di Scienze Farmaceutiche, Università di Salerno, via Ponte don Melillo, 84084, Fisciano (SA), Italy

[§]Physical Chemistry and Mass Spectrometry Laboratory, Department of Chemistry, University of Liège, 4000, Liège, Belgium

[∥]Dipartimento di Chimica Organica e Biochimica

[⊥]Dipartimento di Chimica "P. Corradini"

Università degli Studi di Napoli Federico II, via Cintia, 80126, Napoli, Italy

Supporting Information

ABSTRACT: The cKit87up sequence d($^{5'}$AGGGAGGGCGCTGGGAGGAGGG$^{3'}$) can form a unique G-quadruplex structure in the promoter region of the human c-kit protooncogene. It provides a peculiar platform for the design of selective quadruplex-binding agents, which could potentially repress the protooncogene transcription. In this study, we examined the binding of a small library of PNA probes (**P1**−**P5**) targeting cKit87up quadruplex in either K^+- or NH_4^+-containing solutions by using a combination of UV, CD, PAGE, ITC, and ESI-MS methodologies. Our results showed that (1) **P1**−**P4** interact with the cKit87up quadruplex, and (2) the binding mode depends on the quadruplex stability. In K^+ buffer, **P1**−**P4** bind the ckit87up quadruplex structure as "quadruplex-binding agents". The same holds for P1 in NH_4^+ solution. On the contrary, in NH_4^+ solution, **P2**−**P4** overcome the quadruplex structure by forming PNA/DNA hybrid complexes, thus acting as "quadruplex openers".

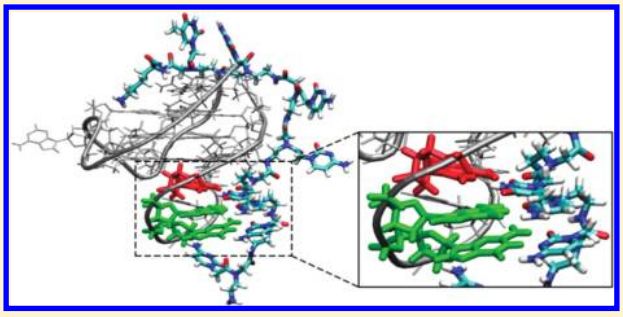

INTRODUCTION

Guanosine-rich nucleic acid sequences have a propensity to form DNA secondary structures, known as G-quadruplexes. These structures are made up of stacked G-tetrad subunits, wherein four coplanar guanines are linked together by Hoogsteen hydrogen bonds.[1] Recent studies have been reported about the high density of putative G-quadruplex-forming sequences in telomeres and in genomic regions adjacent to transcriptional start sites,[2−4] thus supporting the biological importance of these structures *in vivo*.[5−7] Evidence exists that GC-rich regions of gene promoters can transiently unwind and form single-stranded tracts, eventually folding into G-quadruplexes.[8] Hurley and coworkers have provided the direct evidence for a G-quadruplex structure formation in a promoter region of c-MYC and its stabilization with several small molecules, resulting in the repression of c-MYC transcription.[9,10] Two quadruplex-forming sequences have been identified in the promoter region of the c-kit gene. One sequence (c-Kit21) is located within −140 to −160 base pairs (bp) upstream of the transcription initiation site, and the other one (c-Kit87up) between −87 and −109 bp.[11,12] The alteration of c-kit expression has been implicated in a variety of human tumors.[13−16]

These findings suggest that G-quadruplex formation may be related to a general mechanism for gene regulation, and that the modulation of gene expression could be achieved by targeting these structures.[17] Therefore, molecules that selectively bind and stabilize G-quadruplex structures are emerging as attractive gene-related therapeutic agents.[18] A number of ligands able to bind telomeric G-quadruplexes have been investigated for their ability to disable the telomere maintenance in tumor cells,[19] but to date only a few molecules have been investigated for targeting G-quadruplex in gene promoter regions.[20,21]

Very interestingly, NMR analysis of the G-quadruplex structure formed by the 22-mer c-Kit87up sequence has revealed a highly unusual G-quadruplex folding topology.[22] It comprises three G-tetrads with all the guanines in an *anti*-glycosidic conformation and four characteristic loops, one of which comprises five

Received: October 7, 2010
Revised: January 6, 2011
Published: March 16, 2011

residues (Figure 1). Moreover, a bioinformatic study has shown that the c-Kit87up sequence is unique within the human genome.[23]

Among molecules designed to target G-quadruplexes, peptide nucleic acids (PNAs) represent a promising class of synthetic DNA analogues in which the entire sugar−phosphate backbone is replaced by a pseudopeptide.[24] The lower electrostatic repulsion, resulting from the absence of phosphate groups, allows PNAs to form very stable duplexes and triplexes by displacing the cDNA strand in DNA duplexes.[25,26] Strategies usually used for targeting G-rich sequences with PNAs are the formation of PNA/DNA hybrid quadruplexes[27,28] or the induction of G-quadruplex formation by displacing the G-rich/C-rich double-stranded DNA by using short G-rich PNAs that bind to the C-rich strand of DNA.[29]

Herein, we report for the first time the c-Kit87up sequence targeting with PNA probes. Our strategy is based on the identification of PNAs that recognize and stabilize the quadruplex formed by the c-Kit87up sequence. The design and synthesis of short PNAs potentially able to bind to suitable complementary sequences of loops and/or stem regions of the G-quadruplex structure formed by the c-Kit87up sequence are reported. To investigate the physicochemical properties underlying the molecular recognition between the c-Kit87up quadruplex-forming sequence and PNA molecules, circular dichroism (CD) and UV spectroscopies,[30−32] polyacrylamide gel electrophoresis (PAGE), electrospray mass spectrometry (ESI-MS),[33] and calorimetric techniques (ITC)[34] were employed.

EXPERIMENTAL PROCEDURES

Preparation of c-Kit87up Quadruplex and Its Complexes with PNAs. DNA and PNA sequences (Table 1) have been assembled using standard procedures (see Supporting Information).[35−38] The c-Kit87up quadruplex structure (**Q**) was formed by dissolving ckit87up (40 μM) in potassium buffer (10 mM KH_2PO_4, 40 mM KCl, 0.2 mM EDTA, pH = 7.0) or in 150 mM NH_4OAc solution, pH = 7.0 (Sigma Aldrich), and annealed by heating to 90 °C for 5 min followed by slow cooling to room temperature. The quadruplex solutions were then equilibrated at 4 °C for 24 h before addition of the suitable PNA. Each DNA-PNA complex was prepared by mixing equimolar amounts of **Q** and PNA at 25 °C and incubating the resulting mixture for 24 h at the same temperature before data acquisition.

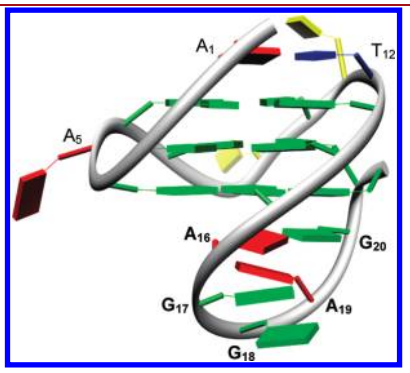

Figure 1. Schematic representation of ckit87up quadruplex structure annealed in K^+-containing solution. Guanine bases are in green, adenines are in red, cytosines are in yellow, and thymine is in blue. The residues belonging to loop-4 are in bold.

Circular Dichroism (CD). CD spectra of DNA, PNA, or mixed solutions (20 μM) were recorded by using a Jasco J-715 spectropolarimeter equipped with a Jasco JPT-423-S temperature controller in the 220−360 nm range, using 1 mm path-length cuvettes. Spectra were averaged over 5 scans, which were recorded at a scan rate of 100 nm/min with a response time of 1 s and a bandwidth of 1 nm. Buffer baseline was subtracted from each spectrum and the spectra were normalized to have zero ellipticity at 360 nm.

Thermal Difference Spectra (TDS) and UV-Melting Experiments. 20 μM solutions of DNA, PNA, and PNA/DNA mixture (0.5 mL) were placed in quartz cuvettes of 0.1 cm path length. Thermal difference spectra and UV-melting experiments were carried out using a Jasco V-530 UV−visible spectrophotometer equipped with a Jasco ETC-505-T temperature controller. TDS were obtained by recording the UV absorbance spectra in the range 220−320 nm at 5 and 90 °C and subsequently taking the difference between the two spectra.[32] UV-melting experiments were performed in the temperature range 5−90 °C by monitoring the absorbance at 295 nm,[31] at a 0.5 °C/min heating rate. The $T_{1/2}$ temperatures were calculated as previously reported by Mergny and Lacroix.[39]

Nondenaturing Polyacrylamide Gel Electrophoresis (PAGE). Nondenaturing gel electrophoreses were performed using 12% polyacrylamide gels, which were run in 1×TBE (Tris-Borate-EDTA) buffer supplemented with 50 mM KCl or 150 mM NH_4OAc, pH 7.0. Bands in the gels were visualized by SYBR Green staining (Sigma-Aldrich). A concentration of 10 μM was used for each sample.

ESI-Mass Spectrometry. ESI-MS studies were conducted using ammonium acetate at pH = 7.0.[33] The experiments were performed on a Q-TOF Ultima Global (Waters, Manchester, UK). The samples (DNA strand concentration = 10 μM) were infused at 4 μL/min in the electrospray source that operated in negative ion mode (capillary voltage = −2.2 kV). The source temperature was 80 °C and the nitrogen desolvation gas temperature was 100 °C. The pressure indicated on the source Pirani gauge was 3.0 mbar. For each sample, spectra were recorded using the following acceleration voltages: a cone voltage of 100 V, a RF Lens 1 voltage of 100 V, and a collision energy voltage (acceleration voltage before the collision hexapole) of 10 V. These voltage values represent a good compromise both to

Table 1. Mass Spectrometry Results of DNA and PNA Sequences Used in This Study[a]

		mass spectrometry results	
molecule	sequence	calculated (MW)	found (MW)
ckit87up	d($^{5'}$AGGGAGGGCGCTGGGAGGAGGG$^{3'}$)	7010.4	$(M+H)^+$ = 7011[b]
P1	H_2N -Lys- tcctc-H	1431.4	$(M+2H)^{2+}$ = 716.7[c]
P2	H_2N -Lys- tcctccc-H	1932.9	$(M+3H)^{3+}$ = 646.1[c]
P3	H_2N -Lys- tccctccc-H	2185.1	$(M+3H)^{3+}$ = 729.3[c]
P4	H_2N -Lys- tccctcccgcgac-H	3544.4	$(M+4H)^{4+}$ = 887.1[c]
P5	H_2N -Lys- ttttttt-H	2276.2	$(M+3H)^{3+}$ = 759.6[c]

[a] All PNA sequences are written from C to N terminus. [b] MALDI-TOF. [c] ESI-MS.

dx.doi.org/10.1021/bc100444v |*Bioconjugate Chem.* 2011, 22, 654–663

preserve the ammonium cations inside the G-quadruplexes and to observe the PNA/DNA complexes.[40] Complexes of higher m/z are not transmitted efficiently at low voltages through the mass spectrometer and, therefore, are not efficiently detected. The spectra were smoothed (2× mean, 10 channels), background-subtracted (polynomial order = 50, 1% below curve), and converted to centroid. The compounds were manually searched with the assistance of the *MassLynx 4.0* software. The average mass was calculated with its standard deviation.

Isothermal Titration Calorimetry (ITC). ITC experiments were performed using a CSC 5300 Nano-ITC microcalorimeter from Calorimetry Science Corporation (Lindon, Utah) with a cell volume of 1 mL. The buffer conditions used for ITC measurements were the same reported for the other experiments. Before each ITC experiment, the reference cell was filled with deionized water, and the DNA solutions were degassed for 5 min to eliminate air bubbles. The experiments were carried out at 25 °C. Care was taken to start the titration after achieving baseline stability. In each titration, volumes of 5−10 μL of a PNA containing solution (80−300 μM) were injected into a solution of quadruplex DNA (10−20 μM) in the same buffer, using a computer-controlled 250 μL microsyringe. The interval between PNA injections was 400 or 500 s. The heat produced by PNAs dilution was evaluated in control experiments by injecting each PNA solution into the buffer alone. The interaction heat for each injection was calculated after correction for the heat of PNA dilution. Measurement from the first injection was discarded from the analysis of the integrated data, in order to avoid artifacts due to the diffusion through the injection port occurring during the equilibration of the baseline. The corrected heat values were plotted as a function of the molar ratio. The integrated heat data were fitted using a nonlinear least-squares minimization algorithm to a theoretical binding isotherm, by means of the Bindwork program supplied with the instrument, to give the binding enthalpy ($\Delta_b H°$), equilibrium binding constant (K_b), and binding stoichiometry (n). The Gibbs energy and the entropic contribution were derived using the relationships $\Delta_b G° = -RT \ln K_b$ ($R = 8.314$ J mol^{-1} K^{-1}, $T =$ 298 K) and $-T\Delta_b S° = \Delta_b G° - \Delta_b H°$.

Molecular Modeling. To obtain a molecular model of the complex between **P3** and ckit87up quadruplex, the NMR solution structure of the quadruplex was used (Protein Data Bank entry number 2O3M), while the molecular model of **P3** was built using the Builder module of *Insight II* package (www.accelrys.com). **P3** was manually placed at a position so that the "$c_2c_3t_4$" bases of PNA form Watson−Crick base pairing with complementary "$A_{16}G_{17}G_{18}$" bases of the loop-4 of **Q**. **P3** backbone was then adapted to the structure of **Q**. The coordinates of the resulting **Q**-**P3** complex were energy minimized under vacuum with the *HyperChem 7.5* software,[41] using the steepest descent method, keeping the DNA residues fixed in position and allowing only the PNA to relax, until convergence to a rms gradient of 0.1 kcal/mol Å was reached.

RESULTS

Evaluation of G-Quadruplex Formation and Stability. The formation of the G-quadruplex structure by the 22-mer ckit87up sequence in potassium or ammonium solution was investigated by using CD, TDS, UV-melting, and PAGE techniques. ESI-MS experiments were also performed according to previous studies.[33,40] The structure formed by ckit87up sequence in the two different cation solutions was evaluated in comparison with that of the unstructured d($^{5'}$CCCTCCTCCCAGCGCCCTCCCT$^{3'}$) 22-mer oligonucleotide by examining the mobility in nondenaturing polyacrylamide gels. Figure 2A shows that **Q** possesses the same mobility in K^+ and NH_4^+ solutions and run faster than the unstructured 22-mer oligonucleotide, thus suggesting that the ckit-87up sequence adopts analogous folding in both the analyzed conditions.

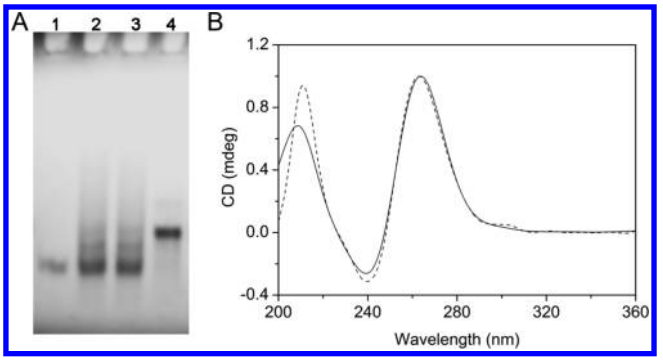

Figure 2. (A) PAGE of **Q** in K^+ and NH_4^+ containing solutions. Lane 1: [d(TGGGGT)]$_4$ in K^+ as quadruplex marker. Lane 2: **Q** annealed in K^+. Lane 3: **Q** annealed in NH_4^+. Lane 4: d($^{5'}$CCCTCCTCCCAGCGCCCTCCCT$^{3'}$) as unstructured 22-mer length marker. (B) Normalized CD spectra of ckit87up sequence annealed in K^+ (solid line) and NH_4^+ (dashed line) solutions.

To obtain a further structural insight into the above G-quadruplex structures,[42] CD spectra of **Q** were recorded either in potassium or in ammonium solution. Both spectra (Figure 2B) show two well-defined maxima around 210 and 263 nm and a minimum at 240 nm, suggesting that the oligonucleotide folds in a parallel-type quadruplex structure in both cases.[30] In addition, thermal difference spectra (TDS) were collected both in K^+ and NH_4^+ solutions. In agreement with CD experiments, the normalized differential absorbance signatures of **Q** show typical patterns of a G-quadruplex structure in both solution conditions (Figure 3, black traces), with two positive maxima at 243 and 273 nm and a negative minimum around 295 nm.[32] The temperature-dependent absorption of quadruplex-forming DNA was monitored at 295 nm (Supporting Information Figure S1). A hypochromic profile, characterized by a single transition, typical of the melting of a quadruplex structure,[31] is observed in both K^+ and NH_4^+ solutions. The thermal stability of **Q** was found to be higher in potassium ($T_{1/2}$ = 47.3 °C) than in ammonium solution ($T_{1/2}$ = 34.3 °C).

To gain information on the number of strands and cations involved in the quadruplex structure, electrospray mass spectrometry experiments were performed. The ckit87up ESI-MS spectrum (Supporting Information Figure S2) shows that the detected main species embeds two ammonium cations in the structure. In agreement with previous studies,[43] ammoniums are better preserved in ions of low charge states.

Evaluation of DNA-PNA Complex Formation. To probe the recognition phenomena between the ckit87up quadruplex-forming sequence and PNA molecules, the interaction of five different PNA sequences (Chart 1) was studied using CD, UV, ESI-MS, PAGE, and ITC techniques.

All the experiments were performed in K^+ and NH_4^+ solutions, except for the ESI-MS analyses that could only be performed in NH_4^+. **P1**−**P4** sequences can potentially target different tracts of the quadruplex structure (**Q**) formed by ckit87up. The 5-mer

P1 is fully complementary to the five bases $A_{16}-G_{20}$ (Figure 1), while **P2** and **P3** are complementary to the last seven and the first eight nucleosides of ckit87up sequence, respectively. The binding properties of these three shorter PNAs were compared to those of a 13-mer PNA strand, **P4**, which is fully complementary to the first thirteen nucleosides of ckit87up. **P2**−**P4** are also complementary to some residues belonging to loop-4 of **Q**. Finally, **P5**, an 8-mer poly-T PNA, noncomplementary to any portion of ckit87up, was used as a control sequence to show that the binding of PNA molecules is sequence specific.

The global structures of complexes formed by adding PNAs (**P1**−**P5**) to the prefolded quadruplex structure **Q**, either in NH_4^+ or in K^+ solutions, were compared by following their mobility on polyacrylamide gels. **Q**+**P1** and **Q**+**P5** mixtures (Figure 4, lanes 3 and 7) show almost the same mobility as **Q** (Figure 4, lane 2), in both potassium and ammonium solutions, while the remaining **Q**+(**P2**−**P4**) mixtures migrate with a lower mobility than **Q** (Figure 4, lanes 4, 5, and 6), thus suggesting the formation of different species.

Figure 5 shows circular dichroism spectra of 1:1 mixtures of **Q** with **P1**−**P4** (**Q**+**P1**, **Q**+**P2**, **Q**+**P3**, and **Q**+**P4**) recorded in potassium (panels A−D) and ammonium (panels E−H) solutions. The spectrum of each mixture is reported in comparison with the arithmetic sum of the individual components. The CD spectrum of **Q**+**P1** mixture recorded in potassium (Figure 5A) was almost identical to the sum of the spectra of the single components, displaying the CD signature characteristic of a parallel-stranded G-quadruplex. The CD spectra of mixtures obtained by adding **P2**, **P3**, or **P4** to **Q** in potassium buffer are all characterized by the maximum at 210 nm—ubiquitous for G-quadruplexes—and show the typical profile observed for parallel-type G-quadruplexes, although a small red-shift (2−5 nm) was observed for the minimum at 240 nm and the maximum at 263 nm (Figure 5, panels B, C, and D). The CD analysis of samples recorded in NH_4OAc solution revealed that the CD profile of the **Q**+**P1** mixture (Figure 5E) is almost superimposable to the sum of the single components, as observed in potassium buffer. Conversely, large changes in the CD spectra were observed upon addition of **P2**−**P4** PNAs to **Q**. Particularly, these mixtures showed significant shifts for the negative minimum (from 240 to 248 nm) and both positive maxima (from 210 to 223 nm and from 263 nm to 270−280 nm; Figure 5, panels F, G, and H). These values, namely, maxima at 223 and 280 nm and minimum at 248 nm, have been previously reported to be characteristic of hybrid PNA-DNA duplex tracts.[44,45] Finally, CD spectra of the **Q**+**P5** mixture recorded in both potassium and ammonium solutions are almost superimposable to the sum of the spectra of the single components, confirming, as expected, that no hybridization occurs in this case (Supporting Information Figure S3).

Figure 3 shows TDS signatures for the complexes formed by mixing equimolar quantities of **Q** and PNAs **P1**−**P4** in potassium buffer (A) and ammonium solution (B). The typical pattern of a G-quadruplex was observed for all the complexes in potassium

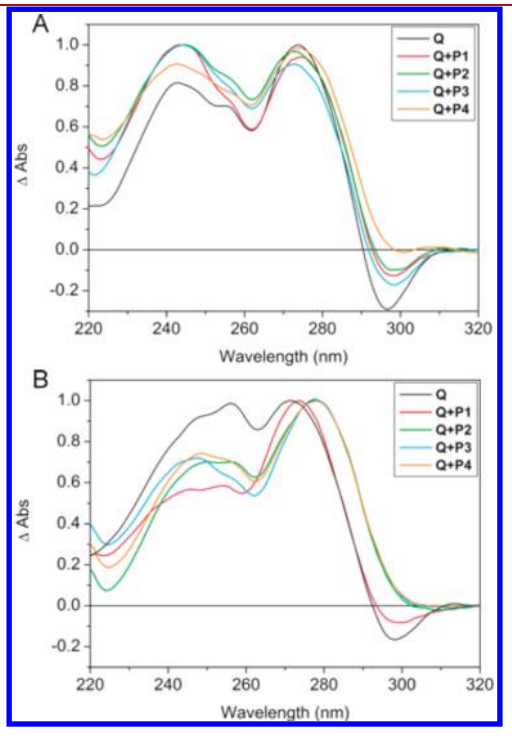

Figure 3. Normalized thermal difference spectra of 1:1 mixtures of **Q** and **Q**+(**P1**−**P4**) in K^+- (A) and in NH_4^+-containing solution (B).

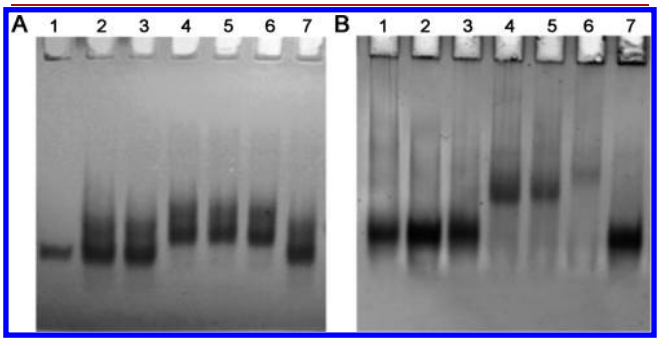

Figure 4. PAGE of 1:1 mixtures of **Q** and **Q**+(**P1**−**P5**), annealed in K^+- (A) and NH_4^+-containing solution (B). Lane 1: $[d(TGGGGT)]_4$ as quadruplex marker. Lane 2: **Q**. Lane 3: **Q**+**P1**. Lane 4: **Q**+**P2**. Lane 5: **Q**+**P3**. Lane 6: **Q**+**P4**. Lane 7: **Q**+**P5**.

Chart 1. Sequences of DNA and PNA Used in This Study[a]

ckit 87up	d(5′AGG-GAG-GGC-GCT-GGG-**AGG-AG**G-G3′)
P1	H_2NLys-t-c-c-t-c-H
P2	H_2NLys-t-c-c-t-c-c-c-H
P3	H_2NLys-t-c-c-c-t-c-c-c-H
P4	H_2NLys-t-c-c-c-t-c-c-c-g-c-g-a-c-H
P5	H_2NLys-t-t-t-t-t-t-t-t-H

[a]Guanines in ckit87up sequences that participate in quadruplex formation are underlined. Residues in loop-4 of **Q** are in bold. DNA sequence is written 5′ to 3′, while the PNA sequences are written C to N terminus.

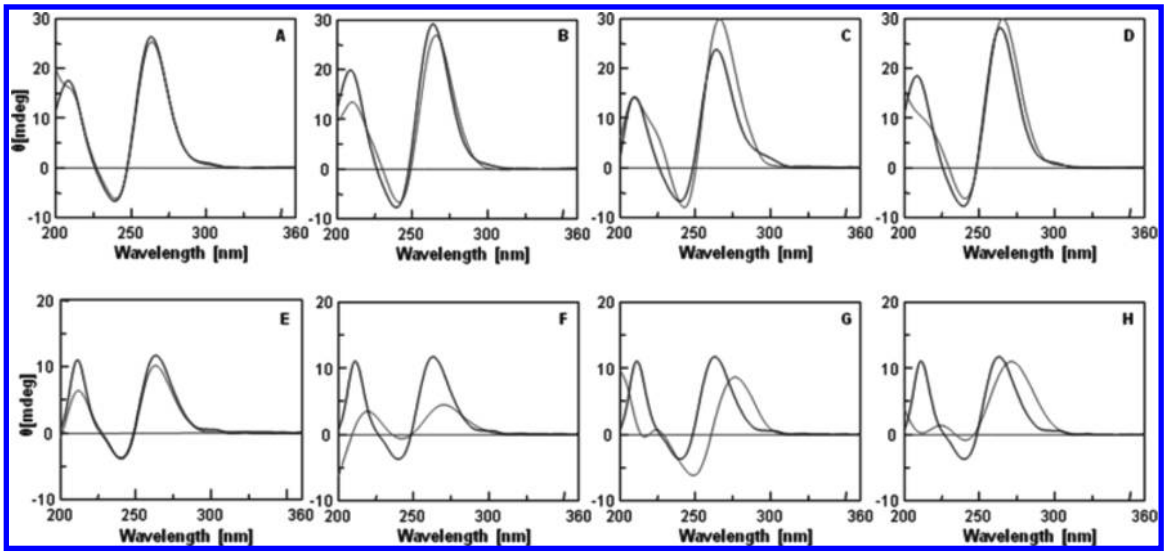

Figure 5. CD spectra of 20 μM **Q** + 20 μM PNAs mixtures (green line) and sum of the spectra of the single components (blue line) in potassium (A−D) and ammonium solution (E−H). **Q**+**P1** (A, E); **Q**+**P2** (B, F); **Q**+**P3** (C, G); **Q**+**P4** (D, H).

buffer. In particular, two positive maxima at 243 and 273 nm, a shoulder at 255 nm, and a negative minimum around 295 nm were observed in all the spectra. Conversely, TDS shapes of PNA-DNA complexes formed in ammonium solution showed the loss of the negative band at 295 nm, except for **Q**+**P1**. Moreover, the positive band at 273 nm was red-shifted to 277 nm, once again except for **Q**+**P1**. The loss of the negative band at 295 nm suggested the absence of Hoogsteen-bonded G-tetrads, while the presence of the peak at 277 nm is compatible with a Watson−Crick duplex-like structure[32] in all **Q**+(**P2**−**P4**) mixtures.

As previously described, a G-quadruplex structure melts with a characteristic hypochromic shift at 295 nm; thus, UV-melting experiments were performed for all the complexes, by recording the absorbance at 295 nm.[31] In potassium buffer, all the UV-melting profiles were consistent with the G-quadruplex foldings (Supporting Information Figure S1). The relative stabilities of PNA-complexed quadruplexes are reported in Table 2. In potassium, all complexes (Supporting Information Figure S1A) displayed $T_{1/2}$ values higher than that of **Q** (ΔT = 2−10 °C), with the exception of **Q**+**P4** for which a destabilizing effect is observed (ΔT = 5.5 °C). On the other hand, in ammonium solution, a hypochromic transition at 295 nm (Supporting Information Figure S1B) is observed only for **Q**+**P1**, once again suggesting the presence of the quadruplex structure. For all other samples, hyperchromic profiles are observed at this wavelength, suggesting the absence of the G-quadruplex scaffold in these complexes.

To better investigate the binding properties shown by the investigated PNA sequences (**P1**−**P4**), a calorimetric analysis of the interaction with **Q** was carried out both in K^+- and in NH_4^+-containing solutions (Figure 6). ITC experiments were also performed by using the poly-T PNA (**P5**, Table 1), as control sequence.

The results collected for titration of **Q** with the five PNAs in K^+ solution reveal that (a) **P1**, **P2**, and **P3** bind to the investigated quadruplex by forming a 1:1 complex; (b) **P4** interacts in a nonspecific manner with **Q**; (c) **P5** does not interact at all. The ITC data for the titrations of **Q** with **P1**, **P2**, and **P3** indicate that the interactions of the PNAs with the quadruplex are favored at 25 °C. However, the characterization of the binding reactions reveals that the interactions of the three PNAs are slightly different from a thermodynamic point of view (Table 4). In all three cases, the binding isotherms indicate exothermic interactions (Figure 6). Indeed, after each injection of PNA, less and less heat release was observed until constant values were obtained, hence reflecting a saturable process. The values of the binding constants clearly show that **P2** and **P3** bind to the investigated quadruplex with higher affinity (K_b = 1 and 3×10^6 M^{-1}, respectively) than **P1** ($K_b = 3 \times 10^5$ M^{-1}). In the cases of **P2** and **P3**, the values of $\Delta_bH°$ and $T\Delta_bS°$ show that the enthalpic contribution provides the driving force for the PNA−quadruplex interaction. However, the interaction of **P3** with **Q** is associated with a larger favorable enthalpy ($\Delta_bH°$ = −110 kJ mol^{-1}) as compared to **P2** ($\Delta_bH°$ = −90 kJ mol^{-1}). On the other hand, the interaction of **P1** is associated with a favorable enthalpic contribution ($\Delta_bH°$ = −12 kJ mol^{-1}) that acts together with the entropic one ($T\Delta_bS°$ = 19 kJ mol^{-1}). The favorable heat observed for the binding reaction is due to the net compensation of the exothermic heat from the formation of base pairs and the endothermic heats of possible H-bonds breaking. In the ITC titrations of **Q** with **P4**, a resolvable binding isotherm was never obtained using several combinations of reactant concentrations,

Table 2. Melting Temperatures for c-Kit87up Quadruplex-Forming Sequence and PNA-DNA Complexes Calculated from UV-Melting Curves Recorded at 295 nm

	$T_{1/2}$ (°C)	
sample	K^+ solution	NH_4^+ solution
Q	47.1 ± 0.1	34.3 ± 0.1
Q+**P1**	49.2 ± 0.2	37.6 ± 0.2
Q+**P2**	54.0 ± 0.2	n.d.
Q+**P3**	56.8 ± 0.2	n.d.
Q+**P4**	41.6 ± 0.2	n.d.

dx.doi.org/10.1021/bc100444v |*Bioconjugate Chem.* 2011, 22, 654–663

not allowing the determination of the thermodynamic parameters or the recognition of a defined stoichiometry. The raw ITC data for the titration of **Q** with **P5** (Supporting Information Figure S4) show constant heat release after each injection of PNA, only due to PNA dilution. A resolvable binding isotherm for the interaction with **Q** is not observed in this case as well, suggesting no affinity of **P5** for the investigated quadruplex.

When the same titrations were performed in the NH_4^+-containing solution, the binding behaviors turned out to be different, except for **P1**. As observed in K^+ solution, **P1** forms a 1:1 complex with **Q**. The thermodynamic parameters (Table 4) indicate that the interaction of **P1** is exothermic ($\Delta_bH° = -13$ kJ mol^{-1}) and it is associated with a favorable entropic contribution ($T\Delta_bS° = 18$ kJ mol^{-1}). On the other hand, the binding curves relative to **P2** and **P3** show less simple profiles compared to the analogous curves in K^+ solution (Figure 6). Indeed, at a molar ratio of 2:1 (PNA/DNA), fluctuating values of heat release were observed after injection of PNA, reflecting a nonsaturated process at that ratio. In NH_4^+ solution, **P4** shows behavior comparable to those of **P2** and **P3**, producing a similar binding profile. In particular, the **P2**−**P4** binding isotherms display a biphasic profile, revealing two consecutive binding events: (1) one PNA molecule interacts with the DNA; (2) a second PNA molecule binds to DNA, leading to the formation of a 2:1 PNA/DNA complex. The interpolation procedure of the experimental data has been carried out with a multiple-sites model. The thermodynamic results obtained from ITC data for **P2**, **P3**, and **P4** binding to DNA are given in Table 4. The thermodynamic characterization of the binding events revealed that the first binding event ($K_b = 2 \times 10^7$ and 3×10^7 M^{-1} for **P2** and **P3**, respectively; $K_b = 8 \times 10^7$ M^{-1} for **P4**) is stronger than the second one ($K_b = 8 \times 10^5$ M^{-1} for both **P2** and **P3**; $K_b = 1 \times 10^6$ M^{-1} for **P4**). Moreover, the analysis indicated that the two binding events are driven by a large enthalpic contribution, while there is an unfavorable entropic contribution.

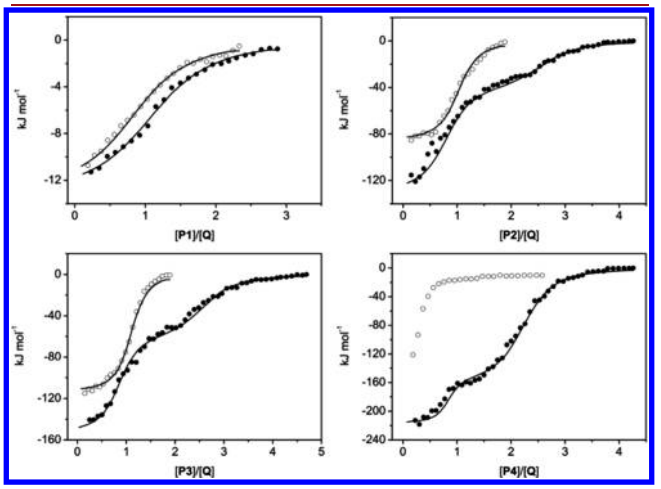

Figure 6. ITC profiles for the interaction between PNA sequences and ckit87up quadruplex in K^+ (open circles) and NH_4^+ (black circles) containing solution. The circles represent the experimental data obtained by integrating the raw data and subtracting the heat of PNA dilution. The lines represent the best-fit curve for the binding.

To establish the molecularity of the complexes in ammonium solution, MS spectra have been acquired by an ESI-Q-TOF instrument under conditions that preserve noncovalent interactions. ESI-MS was previously used to characterize intermolecular PNA/DNA complexes.[46] Here, ESI-MS was used to investigate the stoichiometry of the complexes formed when stoichiometric amounts of **P1**−**P5** are added to **Q** at room temperature (Supporting Information Figure S5). Table 3 summarizes the main species identified from the mass spectra of PNA/DNA complexes. The short **P1** probe interacts with **Q** without disrupting its scaffold, indeed the ESI-MS spectrum shows the presence of the [**Q**-(**P1**)$_1$] adduct with the inner ammoniums preserved (Figure 7). As expected for long PNA sequences, when **P2**−**P4** PNAs are mixed with **Q**, the main peaks observed correspond to 1:1 and 2:1 PNA/DNA hybrid complexes with [**ckit87up**-(**P2**−**P4**)$_1$] > [**ckit87up**-(**P2**−**P4**)$_2$], in agreement with the ITC data. **Q** is less abundant, but always detected. Finally, the **Q**+**P5** spectrum shows no PNA/DNA complex formation, even by increasing PNA concentration (data not shown), thus suggesting that the PNA binding to DNA is sequence specific.

DISCUSSION

The present study reports the first example of PNA probes able to bind to a biologically relevant DNA quadruplex without disrupting its scaffold. While strand invasion of PNA into duplex and quadruplex DNA have been investigated in detail,[47,48] less attention has been paid to the ability of PNA to bind and stabilize the targeted quadruplex. We focused on some different PNA sequences and analyzed their interaction with the quadruplex formed by the ckit87up DNA sequence.

Table 3. Summary of the Peaks Observed in the Electrospray Mass Spectra of ckit87up Quadruplex (Q) + PNAs in 150 mM NH_4OAc at 1:1 DNA/PNA Ratio[a]

	DNA/PNA 1:1		
sample	$\mathbf{Q}^{z-}$ = [ckit87up · $(NH_4^+)_2$]$^{z-}$	[**Q**-(**PNA**)$_n$]$^{z-}$ complex	[**ckit87up**-(**PNA**)$_n$]$^{z-}$ hybrid
Q	$[Q]^{4-\rightarrow5-}$	–	–
Q+**P1**	$[Q]^{4-\rightarrow5-}$ m.p.	[**Q**-(**P1**)$_1$]$^{5-}$	–
Q+**P2**	$[Q]^{4-\rightarrow5-}$ m.p.	–	[**ckit87up**-(**P2**)$_1$] $^{5-\rightarrow6-}$ [**ckit87up**-(**P2**)$_2$] $^{6-\rightarrow7-}$
Q+**P3**	$[Q]^{4-\rightarrow5-}$ l.p.	–	[**ckit87up**-(**P3**)$_1$]$^{4-\rightarrow6-}$ [**ckit87up**-(**P3**)$_2$]$^{5-\rightarrow7-}$
Q+**P4**	$[Q]^{4-\rightarrow5-}$ l.p.	–	[**ckit87up**-(**P4**)$_1$]$^{5-\rightarrow6-}$ [**ckit87up**-(**P4**)$_2$]$^{5-\rightarrow6-}$
Q+**P5**	$[Q]^{4-\rightarrow5-}$	–	–

[a] m.p. = "main product"; l.p. = "low product".

Table 4. Thermodynamic Parameters for the Interaction Between the c-Kit87up Quadruplex-Forming Sequence and PNAs Determined by ITC[a] at 298 K

	first event					second event				
PNA	n	K_b (M^{-1})	$\Delta_bH°$ (kJ mol^{-1})	$T\Delta_bS°$ (kJ mol^{-1})	$\Delta_bG°_{298K}$ (kJ mol^{-1})	n	K_b (M^{-1})	$\Delta_bH°$ (kJ mol^{-1})	$T\Delta_bS°$ (kJ mol^{-1})	$\Delta_bG°_{298K}$ (kJ mol^{-1})
				K^+ solution						
P1	1.0	3×10^5	−12	19	−31					
P2	1.0	1×10^6	−90	−56	−34					
P3	1.0	3×10^6	−110	−73	−37					
				NH_4^+ solution						
P1	1.2	3×10^5	−13	18	−31					
P2	0.9	2×10^7	−130	−88	−42	1.8	8×10^5	−50	−16	−34
P3	0.8	3×10^7	−150	−107	−43	1.8	8×10^5	−60	−26	−34
P4	0.8	8×10^7	−215	−170	−45	1.7	1×10^6	−160	−126	−34

[a] The experimental error for each thermodynamic property is <8%.

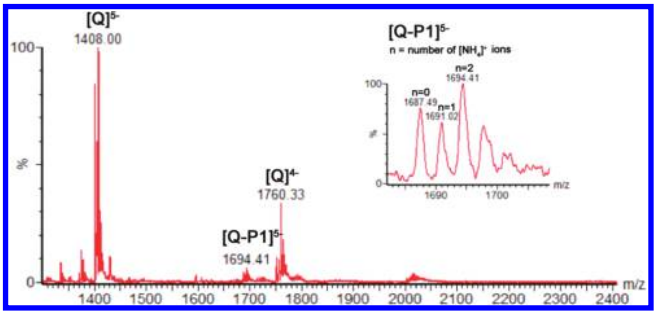

Figure 7. ESI-MS spectra of **Q**+**P1** in 150 mM NH_4OAc. The reported spectrum was acquired in the following soft source conditions: RF Lens1 = 100 V; cone = 100 V; collision energy = 10 V. The inset shows the distribution of the number of ammonium ions remaining in the G-quadruplex (from 0 to 2). [**Q**] = ckit87up quadruplex, namely, [M+2NH_4^+], where M is the single-stranded ckit87up ODN strand; [**Q-P1**] = **Q**+**P1** complex, namely [M+P1 + 2NH_4^+], in which the quadruplex is retained and coordinates two ammonium ions.

In general, the G-quadruplex structures are stabilized by monovalent cations, in particular, K^+ and to a lesser extent Na^+ and NH_4^+.[49] The ckit87up quadruplex predominantly exists in a parallel conformation *in vitro* in K^+ buffer, while in Na^+ solution, it forms aggregated species.[22] NH_4^+ stabilizes G-quadruplexes to an extent comparable with that observed for Na^+, but it displays a coordination geometry similar to that observed for K^+.[50] Therefore, to detect the differences in the molecular recognition process, the analysis was carried out in two different solutions, containing either potassium or ammonium ions.

The PAGE shows very similar behavior for **Q** annealed in K^+- or NH_4^+-containing solution, thus suggesting analogous folding in both ion conditions. Furthermore, ESI-MS data acquired in NH_4^+ solution (the ammonium is the only ion which can be used in the ESI-MS experiments) confirm the quadruplex structure adopted in ammonium showing that two NH_4^+ ions are retained in the quadruplex scaffold (see Supporting Information). In addition, CD and UV data also show the formation of a parallel quadruplex structure in both solutions and, as expected, UV-melting studies revealed that the thermal stability of **Q** in ammonium is lower than that observed in potassium solution.

Binding studies indicate that **P1**−**P4** PNAs are able to bind to ckit87up quadruplex-forming sequence. Interestingly, we observed that the different stability of the quadruplex arrangements affects the binding mode of three (**P2**, **P3**, and **P4**) out of four PNAs.

Our results show that the short **P1** probe binds to **Q** in both NH_4^+ and K^+ solutions without disrupting the target structure. The thermodynamic profiles determined by ITC for the **Q**−**P1** interaction, in the two different solutions, are qualitatively similar. In both cases, the 5-mer PNA binds to the quadruplex, even though with little affinity, and the stoichiometry observed is 1:1. Interestingly, the UV_{295}-melting experiments show that the **Q-P1** complex melts as a quadruplex structure at a temperature quite higher than **Q** alone in both NH_4^+ and K^+ solutions. CD, TDS, and PAGE studies suggested that the structure of the quadruplex is maintained upon **P1** addition in both investigated conditions. ESI-MS analysis confirms this result in ammonium solution. In fact, as for the quadruplex alone, the resulting **Q-P1** complex retains the two ammonium cations embedded in the structure (Figure 7). Since the 5-mer **P1** is complementary to the five bases A_{16}−G_{20} of the long loop-4 of **Q**, it is probably able to bind some of those bases, thus preserving the quadruplex scaffold. Since **Q** and **Q**+**P1** complexes run similarly on the gel, we suppose that the **Q**+**P1** complex retains the overall shape of free **Q**. On the other hand, the binding behavior of **P2**−**P4** PNAs was found to be completely different depending on the cation. Our data indicate that in ammonium solution **P2**−**P4** act as "openers" invading the quadruplex by forming PNA/DNA hybrid complexes. In that solution, the characteristic CD and TDS profiles of the quadruplex are lost upon addition of those PNAs and the typical UV_{295}-melting hypochromic transition of the quadruplex is not more observed. Nondenaturing gel electrophoresis show the formation of different species possessing lower mobility than **Q**, and the results of ESI-MS analysis are compatible with the formation of 1:1 and 2:1 PNA/DNA complexes without ammonium ions embedded, thus confirming that the G-quadruplex scaffold is not retained in these hybrid complexes. The thermodynamic characterization reveals some interesting features about the binding process in ammonium. In particular, ITC data clearly suggest that two consecutive binding events occur when a PNA solution is added in an incremental stepwise fashion to the DNA solution. The first, stronger, binding event has a binding stoichiometry of 1:1, then a weaker second process requiring a much higher PNA concentration for saturation occurs, suggesting that the resulting final complex is composed by two PNA and one DNA strands. The DNA/PNA

dx.doi.org/10.1021/bc100444v |*Bioconjugate Chem.* 2011, 22, 654–663

interaction yielded favorable, enthalpy-driven, free energy contributions, indicating that **P2**−**P4** are able to invade and disrupt the quadruplex structure by forming a stable product. The favorable heat for the first binding reaction is due to the net compensation of exothermic heat attributable to the formation of base-pair stacks and endothermic heat required for breaking the G-tetrad stacks of **Q**. The magnitude of the enthalpy values for the formation of 1:1 and 2:1 PNA/DNA hybrid complexes directly measured in ITC titrations increases by increasing the PNA length and clearly indicates the highest number of base-pair stacks formed in the case of **P4**. Therefore, all the above experiments demonstrate that in ammonium the **P2**, **P3**, and **P4** PNA probes can unfold the quadruplex structure, forming 1:1 and 2:1 PNA/DNA hybrid complexes with the target DNA. Since it is well-known that pyrimidine-rich PNA sequences are able to invade DNA strands by forming PNA-DNA-PNA triplexes, we believe that the 2:1 PNA:DNA complexes, observed in ammonium in the presence of an excess of **P2**, **P3**, and **P4**, can be PNA-DNA-PNA triplex-type complexes.[51]

Conversely, the results of the experiments performed in potassium-containing solution indicate that **P2**−**P4** PNAs are able to bind to **Q**, but none of them overcome the quadruplex structure. Indeed, CD, UV, and PAGE experiments reveal that the structure of the quadruplex is retained upon addition of **P2**, **P3**, or **P4**. Moreover, UV thermal denaturation data indicate that the binding of **P2** and **P3** to **Q** increases the $T_{1/2}$ values of the resulting quadruplex complexes. The energetic profiles, determined by ITC for the binding of **P2** and **P3** to **Q**, are qualitatively comparable, showing, in both cases, a single binding event with a stoichiometry of 1:1. The dissection of the Gibbs energy change into the enthalpy- and entropy-change contributions for the binding shows that the favorable Gibbs energy change is due to a favorable enthalpy change and an unfavorable entropy contribution. The entropy change values observed are the net compensation of (a) the unfavorable entropic contribution, due to the formation of a less relaxed complex with respect to unbounded components, and (b) the favorable entropic contribution, due to the release of coordinated water molecules to the bulk solvent. Moreover, the thermodynamic data revealed that **P3** has a higher affinity for **Q** (K_b for **P3** is three times larger than that for **P2**) and that its interaction is associated with a larger favorable enthalpy change. On the other hand, the ITC titration of **Q** with **P4** shows that the interaction between these molecules does not lead to the determination of thermodynamic parameters associated with a specific interaction.

The overall picture emerging from this study is that the investigated PNAs are able to interact with **Q** in both K^+ and NH_4^+ solutions, but with a different binding mode. As known, the nature of the cations in solution significantly influences the stability of G-quadruplexes. The different behavior of PNA molecules arises just from the relative stability of **Q** in the two ionic solutions. In NH_4^+ solution, the PNAs are able to overcome the less stable quadruplex structure of **Q** hybridizing the DNA sequence. Conversely, in K^+ solution, where the quadruplex structure stability is highest, the PNAs are still able to bind to the quadruplex without overcoming it. The melting experiments of the quadruplex structure in K^+ solution show that the binding of PNAs leads to a stabilization of **Q**, resulting in the following stability order: **Q-P3** > **Q-P2** > **Q-P1**. The ranking orders of binding constants and enthalpies found by ITC are in agreement with the order of thermal stability, and indicate that **P3** is the best quadruplex-binding agent among the investigated PNAs.

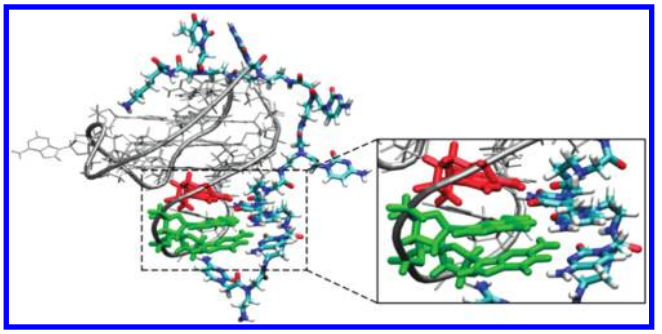

Figure 8. Molecular model of the complex between ckit87up quadruplex (**Q**) and **P3**. **Q** is in gray, and adenine (A_{16}) and guanine (G_{17} and G_{18}) bases involved in Watson−Crick base pairing with the complementary PNA residues are highlighted in red and green, respectively.

The NMR structure of **Q**[22] shows that the only residues potentially able to form Watson−Crick-type base pairs are the bases A_{16}, G_{17}, and G_{18} of the long loop-4; therefore, we speculate that the interaction with PNA involves one of its "c-c-t" stretch. Since **P2** and **P3** bind to **Q** with higher affinity than **P1**, we hypothesize that the best possible interaction occurs with the "c-c-t" motif at the N-terminus. Figure 8 shows a molecular model of **Q-P3** complex, built on the basis of these considerations. The model of the complex shows that the PNA molecule is able to form three Watson−Crick base pairing involving the "$c_2c_3t_4$" bases of **P3** and the complementary "$A_{16}G_{17}G_{18}$" bases. The model also shows that the PNA molecule can adapt its backbone to the structure of **Q**. The flexibility of PNA could allow the positively charged lysine residue to gain additional interactions with the backbone of the quadruplex. The origin of the nonspecific binding of **P4**, that match the C-terminus sequence of **P3**, could be due to the remaining bases at the N-terminus. These latter could also be responsible for the quadruplex destabilization observed in **Q-P4** complex in K^+.

In conclusion, in this paper we proposed a potential way to regulate the c-kit gene transcription by using short PNA sequences. The ckit87up sequence is unique within the human genome, and it folds into an unusual quadruplex structure embodying a peculiar long loop that may represent, as we have shown, the target of new quadruplex-binding agents. Our findings demonstrate that (i) PNAs can act as quadruplex-binding agents, that (ii) their affinity toward the quadruplex depends on PNA sequence and length, and that (iii) the binding mode could be related to the quadruplex stability. These studies open up new routes for the development of improved probes for the regulation of c-kit protooncogene transcription.

■ ASSOCIATED CONTENT

Supporting Information. Experimental procedures for the synthesis of DNA and PNA sequences; UV-melting curves for **Q** and **Q**+(**P1**−**P4**) complexes in potassium and ammonium solution; ESI-MS spectra of **Q** and **Q**+(**P1**−**P5**); CD spectra of **Q**+**P5** in potassium and ammonium solution; ITC data for titration of **Q** with **P5** in potassium solution. This material is available free of charge via the Internet at http://pubs.acs.org.

■ AUTHOR INFORMATION

Corresponding Author

*Tel: +39 081678540. Fax: +39 081678746. E-mail: golivier@unina.it.

Author Contributions

[#]These authors have contributed equally.

■ ACKNOWLEDGMENT

This work was supported by a PRIN grant 2007 from the Italian Ministero dell'Università e della Ricerca [2007EBYL8L_005], by the COST Action MP0802 [STSM5095 to J.A.], by the FRS-FNRS [CC 1.5.286.09 and research associate position to VG] and the University of Liège [FSR starting grant D08/10 to VG]. We would like to thank Dr. Frédéric Rosu and Dr. Luisa Cuorvo for their valuable technical assistance.

■ REFERENCES

(1) Neidle, S. (2009) The structures of quadruplex nucleic acids and their drug complexes. *Curr. Opin. Struct. Biol. 19*, 239–250.

(2) Huppert, J. L., and Balasubramanian, S. (2005) Prevalence of quadruplexes in the human genome. *Nucleic Acids Res. 33*, 2908–2916.

(3) Todd, A. K., Johnston, M., and Neidle, S. (2005) Highly prevalent putative quadruplex sequence motifs in human DNA. *Nucleic Acids Res. 33*, 2901–2907.

(4) Eddy, J., and Maizels, N. (2006) Gene function correlates with potential for G4 DNA formation in the human genome. *Nucleic Acids Res. 34*, 3887–3896.

(5) Shklover, J., Weisman-Shomer, P., Yafe, A., and Fry, M. (2010) Quadruplex structures of muscle gene promoter sequences enhance in vivo MyoD-dependent gene expression. *Nucleic Acids Res. 38*, 2369–2377.

(6) Cogoi, S., Paramasivam, M., Membrino, A., Yokoyama, K. K., and Xodo, L. E. (2010) The KRAS promoter responds to Myc-associated zinc finger and poly(ADP-ribose) polymerase 1 proteins, which recognize a critical quadruplex-forming GA-element. *J. Biol. Chem. 285*, 22003–22016.

(7) Palumbo, S. L., Memmott, R. M., Uribe, D. J., Krotova-Khan, Y., Hurley, L. H., and Ebbinghaus, S. W. (2008) A novel G-quadruplex-forming GGA repeat region in the c-myb promoter is a critical regulator of promoter activity. *Nucleic Acids Res. 36*, 1755–1769.

(8) Sun, D., Guo, K., Rusche, J. J., and Hurley, L. H. (2005) Facilitation of a structural transition in the polypurine/polypyrimidine tract within the proximal promoter region of the human VEGF gene by the presence of potassium and G-quadruplex-interactive agents. *Nucleic Acids Res. 33*, 6070–6080.

(9) Siddiqui-Jain, A., Grand, C. L., Bearss, D. J., and Hurley, L. H. (2002) Direct evidence for a G-quadruplex in a promoter region and its targeting with a small molecule to repress c-MYC transcription. *Proc. Natl. Acad. Sci. U.S.A. 99*, 11593–11598.

(10) Hurley, L. H., Von Hoff, D. D., Siddiqui-Jain, A., and Yang, D. (2006) Drug Targeting of the c-MYC promoter to repress gene expression via a G-quadruplex silencer element. *Semin. Oncol. 33*, 498–512.

(11) Rankin, S., Reszka, A. P., Huppert, J., Zloh, M., Parkinson, G. N., Todd, A. K., Ladame, S., Balasubramanian, S., and Neidle, S. (2005) Putative DNA quadruplex formation within the human c-kit oncogene. *J. Am. Chem. Soc. 127*, 10584–10589.

(12) Fernando, H., Reszka, A. P., Huppert, J., Ladame, S., Rankin, S., Venkitaraman, A. R., Neidle, S., and Balasubramanian, S. (2006) A conserved quadruplex motif located in a transcription activation site of the human c-kit oncogene. *Biochemistry 45*, 7854–7860.

(13) Sakurai, S., Fukasawa, T., Chong, J. M., Tanaka, A., and Fukayama, M. (1999) C-kit gene abnormalities in gastrointestinal stromal tumors (tumors of interstitial cells of Cajal). *Jpn J. Cancer Res. 90*, 1321–1328.

(14) Looijenga, L. H., de Leeuw, H., van Oorschot, M., van Gurp, R. J., Stop, H., Gillis, A., de Gouveia Brazao, C. A., Weber, R. E., Kirkels, W. J., van Dijk, T., and von Lindern, M. (2003) Stem cell factor receptor (c-KIT) codon 816 mutations predict development of bilateral testicular germ-cell tumors. *Cancer Res. 63*, 7674–7678.

(15) Wang, Y. Y., Zhou, G. B., Yin, T., Chen, B., Shi, J. Y., Liang, W. X., Jin, X. L., You, J. H., Yang, G., Shen, Z. X., Chen, J., Xiong, S. M., Chen, G. Q., Xu, F., Liu, Y. W., Chen, Z., and Chen, S. J. (2005) AML1-ETO and C-KIT mutation/overexpression in t(8;21) leukemia: implication in stepwise leukemogenesis and response to Gleevec. *Proc. Natl. Acad. Sci. U.S.A. 102*, 1104–1109.

(16) Fletcher, J. A., and Rubin, B. P. (2007) KIT Mutations in GIST. *Curr. Opin. Genet. Dev. 17*, 3–7.

(17) Kumar, N., Patowary, A., Sivasubbu, S., Petersen, M., and Maiti, S. (2008) Silencing c-MYC expression by targeting quadruplex in P1 promoter using locked nucleic acid trap. *Biochemistry 47*, 13179–13188.

(18) Ou, T. M., Lu, Y. J., Tan, J. H., Huang, Z. S., Wong, K. Y., and Gu, L. Q. (2008) G-quadruplexes: Targets in anticancer drug design. *ChemMedChem 3*, 690–713.

(19) Pagano, B., and Giancola, C. (2007) Energetics of quadruplex-drug recognition in anticancer therapy. *Curr. Cancer Drug Targets 7*, 520–540.

(20) Gunaratnam, M., Swank, S., Haider, S. M., Galesa, K., Reszka, A. P., Beltran, M., Cuenca, F., Fletcher, J. A., and Neidle, S. (2009) Targeting human gastrointestinal stromal tumor cells with a quadruplex-binding small molecule. *J. Med. Chem. 52*, 3774–3783.

(21) Bejugam, M., Sewitz, S., Shirude, P. S., Rodriguez, R., Shahid, R., and Balasubramanian, S. (2007) Trisubstituted isoalloxazines as a new class of G-quadruplex binding ligands: small molecule regulation of c-kit oncogene expression. *J. Am. Chem. Soc. 129*, 12926–12927.

(22) Phan, A. T., Kuryavyi, V., Burge, S., Neidle, S., and Patel, D. J. (2007) Structure of an unprecedented G-quadruplex scaffold in the human c-kit promoter. *J. Am. Chem. Soc. 129*, 4386–4392.

(23) Todd, A. K., Haider, S. M., Parkinson, G. N., and Neidle, S. (2007) Sequence occurrence and structural uniqueness of a G-quadruplex in the human c-kit promoter. *Nucleic Acids Res. 35*, 5799–5808.

(24) Nielsen, P. E., Egholm, M., Berg, R. H., and Buchardt, O. (1991) Sequence-selective recognition of DNA by strand displacement with a thymine-substituted polyamide. *Science 254*, 1497–1500.

(25) Nielsen, P. E., and Christensen, L. (1996) Strand displacement binding of a duplex-forming homopurine PNA to a homopyrimidine duplex DNA target. *J. Am. Chem. Soc. 118*, 2287–2288.

(26) Zhang, X., Ishihara, T., and Corey, D. R. (2000) Strand invasion by mixed base PNAs and a PNA-peptide chimera. *Nucleic Acids Res. 28*, 3332–3338.

(27) Roy, S., Tanious, F. A., Wilson, W. D., Ly, D. H., and Armitage, B. A. (2007) High-affinity homologous peptide nucleic acid probes for targeting a quadruplex-forming sequence from a MYC promoter element. *Biochemistry 46*, 10433–10443.

(28) Paul, A., Sengupta, P., Krishnan, Y., and Ladame, S. (2008) Combining G-quadruplex targeting motifs on a single peptide nucleic acid scaffold: a hybrid (3 + 1) PNA-DNA bimolecular quadruplex. *Chemistry 14*, 8682–8689.

(29) Onyshchenko, M. I., Gaynutdinov, T. I., Englund, E. A., Appella, D. H., Neumann, R. D., and Panyutin, I. G. (2009) Stabilization of G-quadruplex in the BCL2 promoter region in double-stranded DNA by invading short PNAs. *Nucleic Acids Res. 37*, 7570–7580.

(30) Kypr, J., Kejnovska, I., Renciuk, D., and Vorlickova, M. (2009) Circular dichroism and conformational polymorphism of DNA. *Nucleic Acids Res. 37*, 1713–1725.

(31) Mergny, J. L., Phan, A. T., and Lacroix, L. (1998) Following G-quartet formation by UV-spectroscopy. *FEBS Lett. 435*, 74–78.

(32) Mergny, J. L., Li, J., Lacroix, L., Amrane, S., and Chaires, J. B. (2005) Thermal difference spectra: a specific signature for nucleic acid structures. *Nucleic Acids Res. 33*, e138.

(33) Rosu, F., De Pauw, E., and Gabelica, V. (2008) Electrospray mass spectrometry to study drug-nucleic acids interactions. *Biochimie 90*, 1074–1087.

(34) Pagano, B., Mattia, C. A., and Giancola, C. (2009) Applications of isothermal titration calorimetry in biophysical studies of G-quadruplexes. *Int. J. Mol. Sci. 10*, 2935–2957.

(35) Matteucci, M. D., and Caruthers, M. H. (1981) Synthesis of deoxyoligonucleotides on a polymer support. *J. Am. Chem. Soc. 103*, 3185–3191.

(36) Beaucage, S. L., and Caruthers, M. H. (1981) Deoxynucleoside phosphoramidites--A new class of key intermediates for deoxypolynucleotide synthesis. *Tetrahedron Lett. 22*, 1859–1862.
(37) McBride, L. J., and Caruthers, M. H. (1983) An investigation of several deoxynucleoside phosphoramidites useful for synthesizing deoxyoligonucleotides. *Tetrahedron Lett. 24*, 245–248.
(38) Christensen, L., Fitzpatrick, R., Gildea, B., Petersen, K. H., Hansen, H. F., Koch, T., Egholm, M., Buchardt, O., Nielsen, P. E., Coull, J., and Berg, R. H. (1995) Solid-phase synthesis of peptide nucleic acids. *J. Pept. Sci. 3*, 175–183.
(39) Mergny, J. L., and Lacroix, L. (2003) Analysis of thermal melting curves. *Oligonucleotides 13*, 515–537.
(40) Smargiasso, N., Rosu, F., Hsia, W., Colson, P., Baker, E. S., Bowers, M. T., De Pauw, E., and Gabelica, V. (2008) G-quadruplex DNA assemblies: Loop length, cation identity, and multimer formation. *J. Am. Chem. Soc. 130*, 10208–10216.
(41) *HyperChem 7.5*; Hypercube, Inc.; Gainesville, FL, 2002.
(42) Paramasivan, S., Rujan, I., and Bolton, P. H. (2007) Circular dichroism of quadruplex DNAs: Applications to structure, cation effects and ligand binding. *Methods 43*, 324–331.
(43) Gabelica, V., Baker, E. S., Teulade-Fichou, M. P., De Pauw, E., and Bowers, M. T. (2007) Stabilization and structure of telomeric and c-myc region intramolecular G-quadruplexes: The role of central cations and small planar ligands. *J. Am. Chem. Soc. 129*, 895–904.
(44) Ganesh, K. N., and Nielsen, P. E. (2000) Peptide nucleic acids: Analogs and derivatives. *Curr. Org. Chem. 4*, 931–943.
(45) Kushon, S. A., Jordan, J. P., Seifert, J. L., Nielsen, H., and Armitage, B. A. (2001) Effect of secondary structure on the thermodynamics and kinetics of PNA hybridization to DNA hairpins. *J. Am. Chem. Soc. 123*, 10805–10813.
(46) Amato, J., Oliviero, G., De Pauw, E., and Gabelica, V. (2009) Hybridization of short complementary PNAs to G-quadruplex forming oligonucleotides: An electrospray mass spectrometry study. *Biopolymers 91*, 244–255.
(47) Kushon, S. A., Jordan, J. P., Seifert, J. L., Nielsen, H., Nielsen, P. E., and Armitage, B. A. (2001) Effect of secondary structure on the thermodynamics and kinetics of PNA hybridization to DNA hairpins. *J. Am. Chem. Soc. 123*, 10805–10813.
(48) Datta, B., and Armitage, B. A. (2001) Hybridization of PNA to structured DNA targets: quadruplex invasion and the overhang effect. *J. Am. Chem. Soc. 123*, 9612–9619.
(49) Hardin, C. C., Perry, A. G., and White, K. (2000) Thermodynamic and kinetic characterization of the dissociation and assembly of quadruplex nucleic acids. *Biopolymers 56*, 147–194.
(50) Schultze, P., Hud, N. V., Smith, F. W., and Feigon, J. (1999) The effect of sodium, potassium and ammonium ions on the conformation of the dimeric quadruplex formed by the Oxytricha nova telomere repeat oligonucleotide d(G(4)T(4)G(4)). *Nucleic Acids Res. 27*, 3018–3028.
(51) Ray, A., and Nordén, B. (2000) Peptide nucleic acid (PNA): its medical and biotechnical applications and promise for the future. *FASEB J. 14* (9), 1041–1060.